

Slide 1

Mechanisms of emerging disease

Mechanisms

- Change in pathogen
- Release of pathogen into naïve population
 - Movement of animals
 - Movement of animal products
- Expansion of population into new territory
- Climate change (change in global environment)
 - Altered pathogen-host dynamics
 - Altered vector dynamics
 - Altered food availability*
 - Altered toxin exposure*
- Change in local environment
 - Human:domestic:wildlife interface*

Slide 3



Change in pathogen

Slide 4



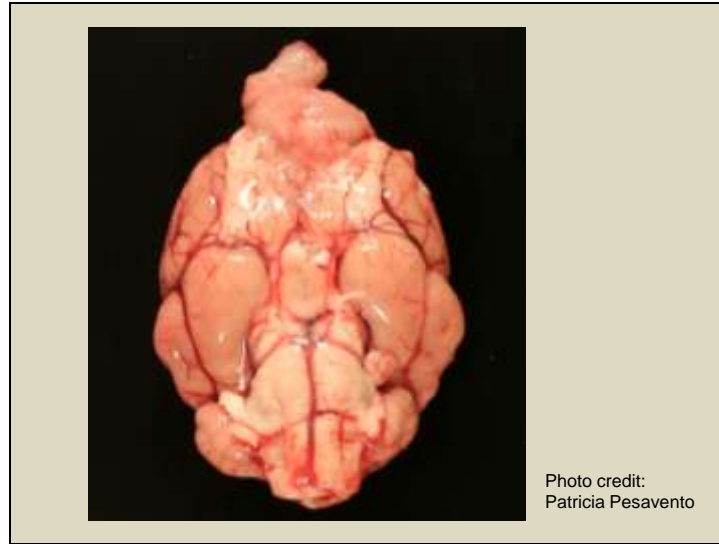
Slide 5



From March 2010 to May 2012, 52 raccoons were submitted to the California Animal Health and Food Safety Laboratory at UC Davis for rabies screening and full necropsy as part of the state diagnostic protocol. Upon examining the brain, 10 of these raccoons were discovered to have brain and/or olfactory tumours. Nine of the animals came from northern California and one from southern Oregon. In all cases, the animals were exhibiting neurologic signs including emerging in the daytime, approaching people or lack of consciousness. In general, other tissues were within normal limits. (Dela Cruz *et al.* 2013)

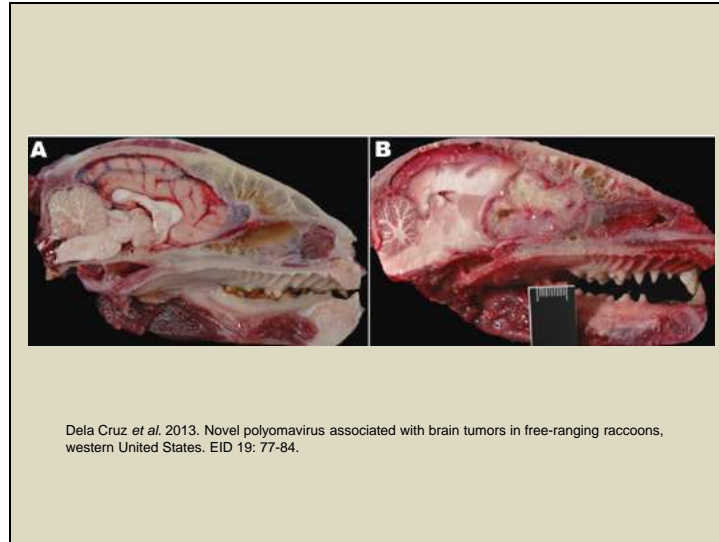
The authors of this report thought this incidence rate was high (yep, agreed!) but to confirm this they performed a retrospective case search and literature search throughout the US and Canada and found only 2 reports of primary brain tumours in approximately 700 examined raccoons.

Slide 6



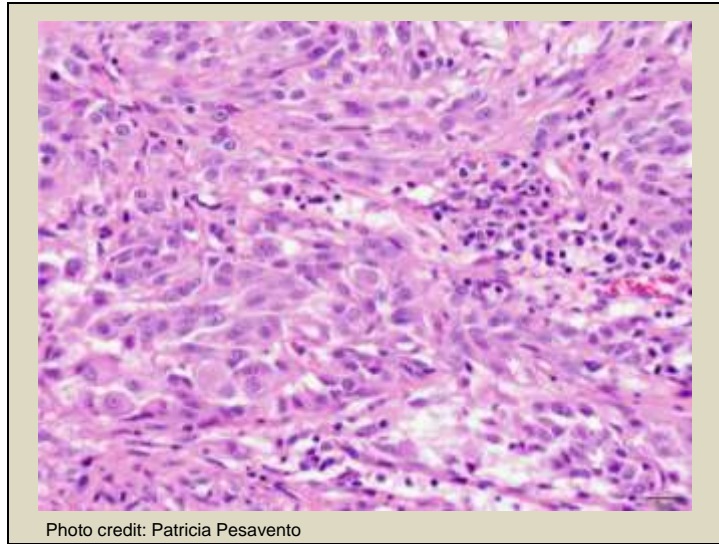
In all cases but one, the tumour involved the cranial portion of one or both frontal lobes.

Slide 7



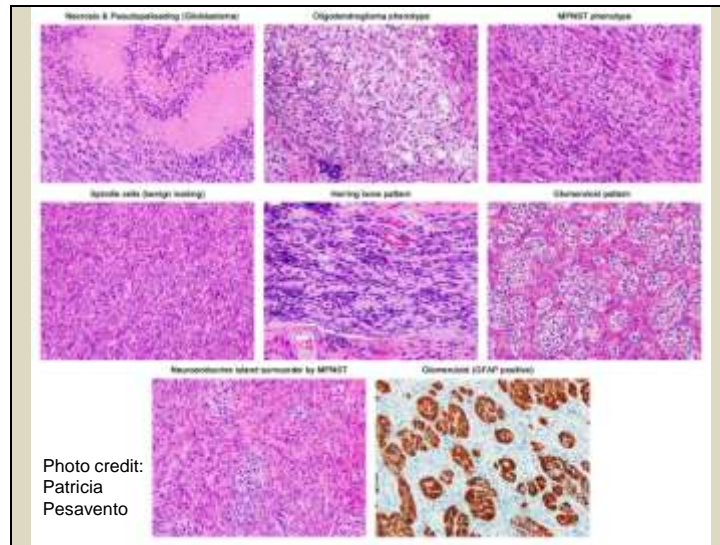
In most cases, the mass spanned the cribriform plate of the ethmoid bone and was continuous with the olfactory tract. In the one case in which a mass was not detectable grossly, the tumour was exclusively localised within the olfactory tract and segments of the axonal bundles of olfactory nerves within the ethmoid turbinates. This was thought to be an early tumour and therefore suggested to the authors that this was possibly the site of origin (Dela Cruz *et al.* 2013)

Slide 8



In some cases the tumours were highly anaplastic, as is the case here.

Slide 9



Most of the original tumours were histologically pleomorphic, but were classified as either malignant peripheral nerve sheath tumours or glioblastomas based on anatomic location, histopathology and immunohistochemistry.

Glioblastomas all expressed glial fibrillary acidic protein, had variable areas of necrosis and high mitotic activity

MPNSTs also expressed GFAP, but the neoplastic cells were also individually surrounded by a reticulin-positive framework which was immunoreactive with laminin.

Viral inclusions were not seen histologically and no viral particles were found on EM (Dela Cruz *et al.* 2013).

Slide 10

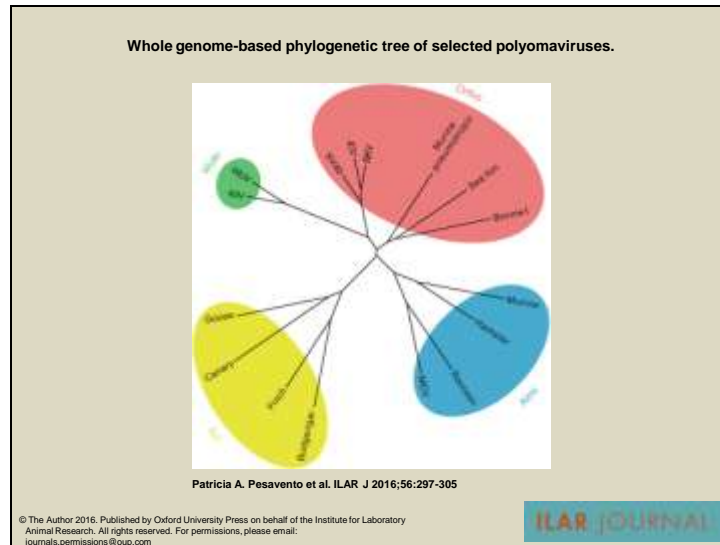


This image demonstrates the tumour crawling along the olfactory tract (nuclear streaming is an artifact of freeze/thaw).

Differentials

- Cluster of cases – point source
 - Environmental toxin
 - Radiation
 - Recent genetic mutation
 - Infectious

Slide 12



Whole genome-based phylogenetic tree of selected polyomaviruses. Polyomaviruses cluster into four distinct groups based on whole nucleotide sequences: avipolyomaviruses, almipolyomaviruses, orthopolyomaviruses, and wukipolyomaviruses (Pesavento *et al.* 2015).

JC virus is a human polyomavirus which has been associated with brain tumours including a broad range of glial tumours.

Authors developed primers based on JCV and were able to identify a new polyomavirus within the raccoon tumours, which they have subsequently named raccoon polyomavirus. They were unable to detect this virus in brain tissue or multiple other tissues in unaffected raccoons from the same geographical area. Therefore, they suggest that raccoon polyomavirus may be involved in the development of these tumours (Pesavento *et al.* 2015).

Update

- As of early 2016 20/240 (8%)
- Bulk of the tumours are PNST type
- Have identified the cell of origin as a stem cell that repopulates the olfactory tract
- Raccoons all over US are seropositive

Pesavento *et al.* 2015. Polyomavirus and naturally occurring neuroglial tumors in raccoons (*Procyon lotor*). *ILAR Journal* 56:297-305.

Seropositivity

- Overall, North American raccoons – 36%
- Californian raccoons – 62%
- So:
 - When were raccoons first infected with RacPyV?
 - Is this virus truly involved in tumorigenesis?
 - If so, what factor is triggering cellular transformation?

- We (UC Davis in collaboration with NIH and UCSF) have, at this point, an algorithm using molecular biology (deg PCR, deep sequencing, RCA etc) to find viruses associated with tumors, so if anyone there has a candidate tumor they want us to work up, let us know!

Patricia Pesavento
papesavento@ucdavis.edu

References

- Dela Cruz *et al.* 2013. Novel polyomavirus associated with brain tumors in free-ranging raccoons, western United States. *Emerging Infectious Diseases* 19:77-84.
- Pesavento *et al.* 2015. Polyomavirus and naturally occurring neuroglial tumors in raccoons (*Procyon lotor*). *ILAR Journal* 56:297-305.

Release of pathogen into naïve
population

Movement of animals



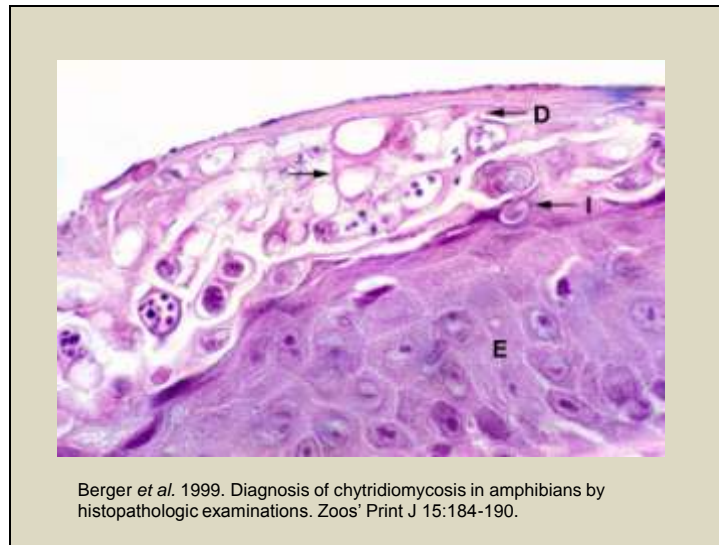
Endangered Sierra Nevada yellow-legged frog for which chytrid infection has played a role in its decline. Happily, following efforts to remove introduced predators, numbers appear to be increasing in the face of chytridiomycosis (Knapp *et al.* 2016).

Chytridiomycosis

- Late 1970s, die-offs of amphibians, primarily in Central America and Australia
- Eventually an infectious disease was suspected and the next site of infection was predicted. Close monitoring allowed the culprit to be discovered: *Batrachochytrium dendrobatidis*
- Chytridiomycosis is now recognised as the most devastating disease on record to impact vertebrate diversity



Gross signs are minimal with sloughing of thickened keratinized layers of skin most apparent. Clinically, frogs are lethargic and anorexic, have abnormal posture with extended hind legs and lose their righting reflex. The mechanism for these clinical signs and ultimate death appears to be impaired electrolyte transfer with cardiac arrest occurring ultimately.



Chytrid infected skin becomes hyperplastic and hyperkeratotic with proliferation of the corneal layer to upto 30x normal thickness.

Histology of a skin section from a White's treefrog (Litoria caerulea), showing heavy chytrid infection.

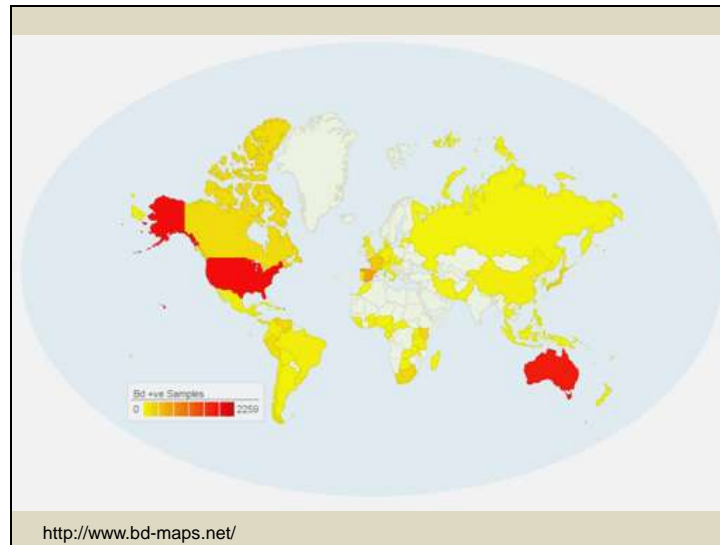
Figure legend:

I: immature stage of zoosporangium.

D: mature zoosporangium containing zoospores, where discharge papillum is visible.

Arrow: empty zoosporangium, after zoospores have discharged.

E: epidermis.



Countries where Bd testing has occurred and the number of positive samples. Online this is an interactive map. Red countries include: Australia, US, Puerto Rico; next highest countries are Spain, France, Japan, Canada, South Africa, Kenya and Venezuela which all have over 200 positive samples. Countries in white have not sampled.

In most locations, chytrid appears to be a new arrival, as is evidenced by marked genetic similarity between samples from different countries and continents. Some exceptions to this do occur, such as in Japan where there is much greater diversity in chytrid genetics and frogs seem less susceptible to infection and/or death from infection. This supports the idea of new introductions, rather than changed environmental factors to explain the emergence of this disease.

How is chytridiomycosis being spread?

- Transport of infected amphibians
 - Food industry, pet trade, scientific trade, bait trade, accidental
- Transport of infected material
 - Water, soil
- Transport by other animals
 - Crayfish, feet of birds
- Climate change?

Table 2. Cumulative Bd and Ranavirus detection in amphibians imported from Hong Kong.

Species	Common Name	# Bd	Bd +	# RV	RV + H ₂ O _{Bd} +	Sloughing	Ulcers	DOA
<i>Bombina orientalis</i>	Oriental Fire							
	Bellied Toad	56	3	13	10	-	22	0
<i>Cynops orientalis</i>	Oriental Fire							
	Bellied Newt	97	0	78	60	-	7	4
<i>Paramesotriton hongkongensis</i>	Hong Kong							
	Newt	72	0	54	35	+	8	0
<i>Xenopus laevis</i>	African							
	Clawed Frog	40	28	40	0	+	0	0
		265	31	185	105		37	4
							23	

Number of individuals sampled (#) for either *Bd* or ranavirus (RV), number of individuals testing positive by PCR (+), and presence of pathogen in water (H₂O_{Bd}+) are expressed. Animal condition recorded upon sampling is provided, including skin sloughing, ulceration, and the number of skin samples that were dead on arrival (DOA)
doi:10.1371/journal.pone.0090750.t002

Kolby JE, Smith KM, Berger L, Karesh WB, Preston A, et al. (2014) First Evidence of Amphibian Chytrid Fungus (*Batrachochytrium dendrobatidis*) and Ranavirus in Hong Kong Amphibian Trade. PLOS ONE 9(3): e90750. doi:10.1371/journal.pone.0090750
<http://journals.plos.org/plosone/article?id=10.1371/journal.pone.0090750>

PLOS ONE
TENTH ANNIVERSARY

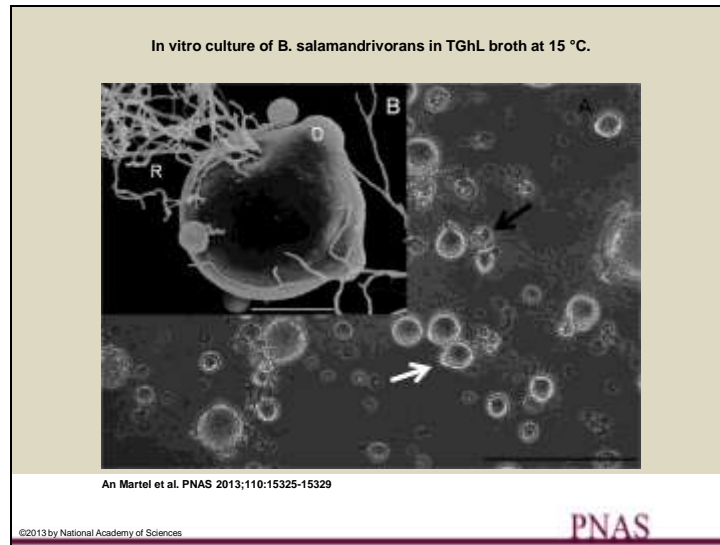
Approximately 720,000 live amphibians were exported from Hong Kong and imported into the USA annually from 2006–2010. Although exported amphibians were primarily documented to have been bred in captivity in Hong Kong, some were first imported from other southeast Asian countries such as China, Indonesia, Singapore, and Thailand, and then re-exported from Hong Kong to the USA. In this study, Kolby *et al.* (2014) tested frogs and salamanders arriving in the US from Hong Kong. Analysis of skin (*Bd*) and cloacal (ranavirus) swabs by quantitative PCR detected pathogen presence in 31/265 (11.7%) and in 105/185 (56.8%) of amphibians, respectively. In addition, the water in which animals were transported tested positive for *Bd*, demonstrating the risk of pathogen pollution by the disposal of untreated wastewater (Kolby *et al.* 2014).

An analysis of trade activity from 2005–2006 showed the importation of nearly 4.3 million live amphibians into Hong Kong, comprised of at least 45 species originating from 11 countries, nine of which have reported presence of *Bd* and/or ranavirus in wild or traded herptiles (Kolby *et al.* 2014).



Since 2010, the fire salamander population of the Netherlands has been undergoing a dramatic reduction, such that by 2013 only 4% of the original population was believed to remain. In 2012, half of a population brought into captivity as a conservation measure died over the course of two months. Affected salamanders died within 7 days, first demonstrating anorexia, apathy and ataxia. They exhibited multifocal superficial erosions and deep ulcerations all over the body.

Testing for a variety of infectious agents, including *B. dendrobatidis* proved negative.



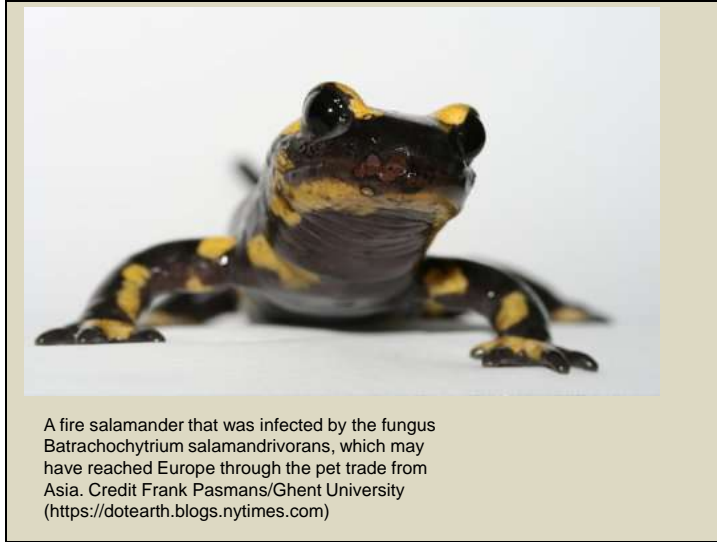
However, this guy was cultured. This is *Batrachochytrium salamandrivorans*, a newly discovered member of the fungal phylum Chytridiomycota.

In vitro culture of *B. salamandrivorans* in TGhL broth at 15 °C. (A) Monocentric thalli predominate, with the rare presence of colonial thalli (black arrow). Sporangia develop discharge tubes (white arrow) to release zoospores (scale bar, 100 μm .) (B) Scanning electron microscopic image of a mature sporangium with rhizoids (R), discharge tubes (D), and germ tube formation (arrow) (Scale bar, 10 μm .) (Martel et al, 2013).

Slide 27



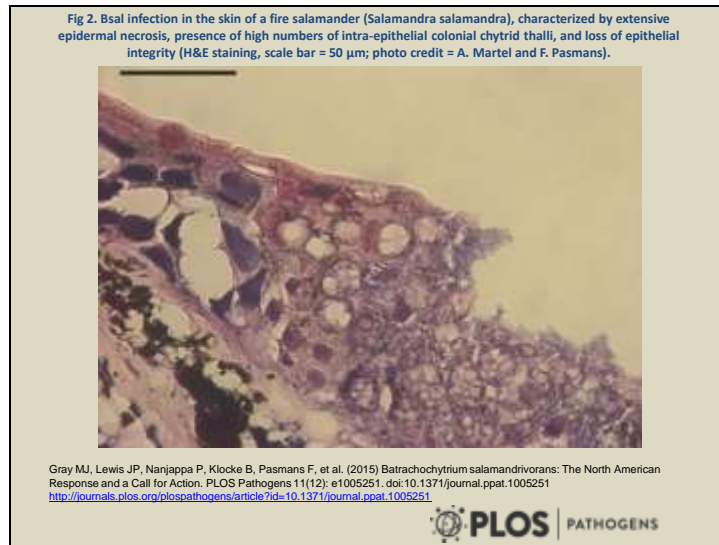
In contrast to *B. dendrobatidis*, there are highly visible gross changes on the skin of these salamanders.



A fire salamander that was infected by the fungus *Batrachochytrium salamandrivorans*, which may have reached Europe through the pet trade from Asia. Credit Frank Pasmans/Ghent University (<https://dotearth.blogs.nytimes.com>)



Lesions caused by the fungus Bsal, as in this wild fire salamander from Belgium, can lead to a gooey death in three to four days. (Photos © Mark Blooi) (<http://news.berkeley.edu>)

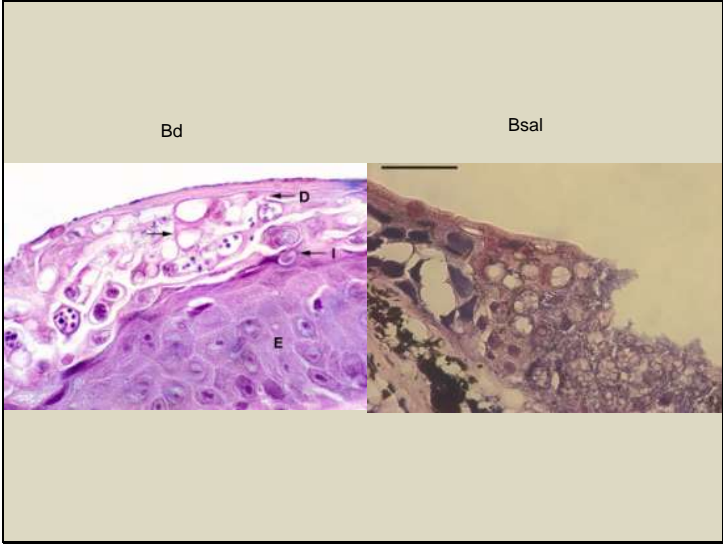


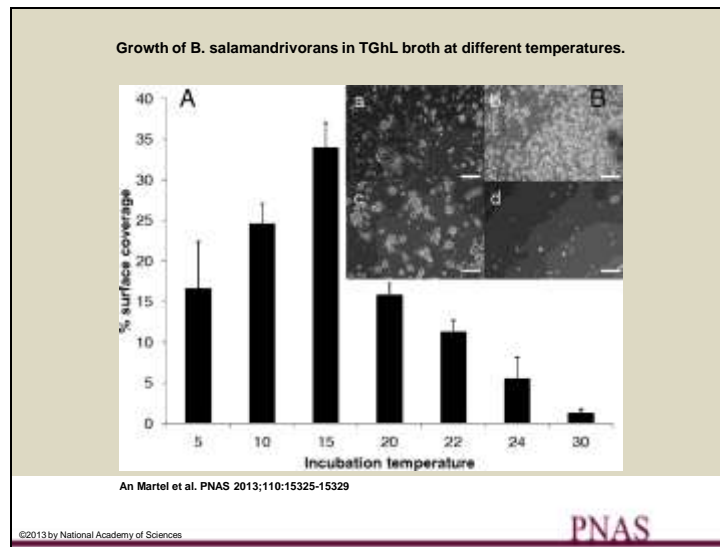
The ulceration seen with *B. salamandrivorans* infection is different from *B. dendrobatidis* in which the lesions generally consist of epidermal hyperplasia and hyperkeratosis.

Keratinocytes with eosinophilic necrosis and marginated nuclei were at the periphery of erosions. Each of these keratinocytes contained one centrally located thallus, the majority of which were segmented or so called colonial thalli, which is different from *B. dendrobatidis* (Martel *et al*, 2013).



Microscopy of the skin of a fire salamander that died due to infection with *B. salamandrivorans*. (A) Immunohistochemical staining of a 5- μm skin section. Intracellular colonial thalli abound throughout all epidermal cell layers and are associated with erosive lesions. (Scale bar, 20 μm .) (B) Transmission electron microscopy picture of an intracellular colonial thallus of *B. salamandrivorans* inside a keratinocyte (Scale bar, 4 μm .) (Martel *et al*, 2013).

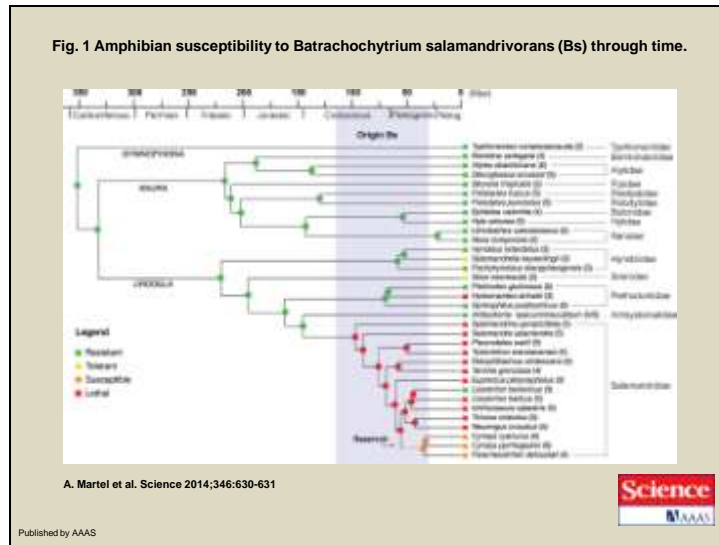




Interestingly, attempts to infect midwife toads, the European species most susceptible to *B. dendrobatidis* were unsuccessful, indicating a different host species range for this pathogen.

Bsal grew at temperatures as low as 5°C, with optimal growth between 10 and 15°C and death at $\geq 25^\circ\text{C}$, a markedly lower thermal preference compared with *B. dendrobatidis* (Martel et al, 2013).

Growth of *B. salamandrivorans* in TGHl broth at different temperatures. (A) Growth was quantified by calculating the average percentage \pm SD of the surface area of three wells covered by the fungus after 10 d of incubation at a given temperature. Motile zoospores were present at 5–20°C, but not at 22, 24, and 30°C. (B) *B. salamandrivorans* growth after 10 d at 4°C (a), 15°C (b), 20°C (c), and 30°C (d) (Scale bar, 200 μm). (Martel et al, 2013).



Amphibian susceptibility to *Batrachochytrium salamandrivorans* (Bs) through time. Molecular time scale (millions of years ago) for 34 species; rectangles indicate the species category based on the experimental infection tests. Resistant: no infection, no disease; tolerant: infection in the absence of disease; susceptible: infection resulting in clinical disease with possibility of subsequent recovery; lethal: infection resulting in lethal disease in all infected animals. Colored dots on nodes indicate the results of the maximum likelihood ancestral reconstructions ($P > 0.95$). The clade of susceptible Asian salamanders that originated in the early Paleogene is indicated in orange. The 95% highest posterior density for time of divergence between *B. salamandrivorans* and *B. dendrobatidis* is indicated in gray (Martel *et al*, 2014).

B sal in Australia

- Currently no testing available in Australia
- Current research indicates frogs are not susceptible (frogs only native amphibs in Aus)
- No pet trade in amphibians

References

- Berger *et al.* 1999. Diagnosis of chytridiomycosis in amphibians by histopathologic examinations. *Zoos' Print J* 15:184-190.
- Berger *et al.* 2016. History and recent progress on chytridiomycosis in amphibians. *Fungal ecology* 19:89-99.
- Gray *et al.* 2015. *Batrachochytrium salamandrivorans*: The North American Response and a Call for Action. *PLOS Pathogens* 11(12): e1005251. doi:10.1371/journal.ppat.1005251
- Knapp *et al.* 2016. Large-scale recovery of an endangered amphibian despite ongoing exposure to multiple stressors. *PNAS* 113:11889-11894
- Martel *et al.* 2013. *Batrachochytrium salamandrivorans* sp. nov. causes lethal chytridiomycosis in amphibians. *PNAS* 110:15325-15329.
- Martel *et al.* 2014. Recent introduction of a chytrid fungus endangers Western Palearctic salamanders. *Science* 346:630-631
- Yap *et al.* 2015. Averting a North American biodiversity crisis - A newly described pathogen poses a major threat to salamanders via trade. *Science* 349:481-482.

Release of pathogen into naïve
population

Movement of animal products



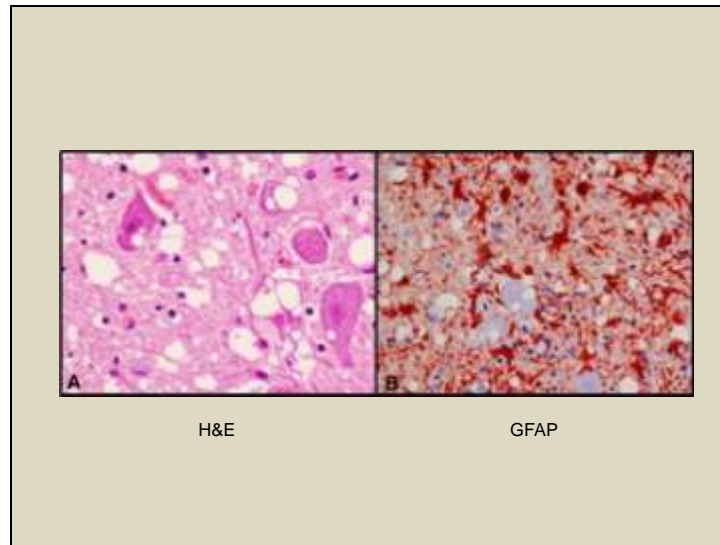
In contrast to the emergence of diseases due to the movement of infected animals, there are also suggestions that the movement of animal products can release a pathogen into a naïve population. This may have been the case in this next disease.



Our next story takes us to southern Norway to the Nordfella population of free-ranging reindeer.

Gross and histo findings

- Poor body condition despite not being pregnant
- Acute exertional (capture) myopathy
- Aspiration pneumonia
- Vacuolation of the neuropil and neurons of the obex, particularly the dorsal motor nucleus of the vagus nerve



Histology of the obex. **A** HE staining showing vacuoles in the neurons and neuropil $\times 600$. **B** Glial fibrillary acidic protein (GFAP) immunolabelling showing strong proliferation of reactive astrocytes (gliosis) in the obex area $\times 400$ (Benestad *et al* 2016).

Ancillary testing

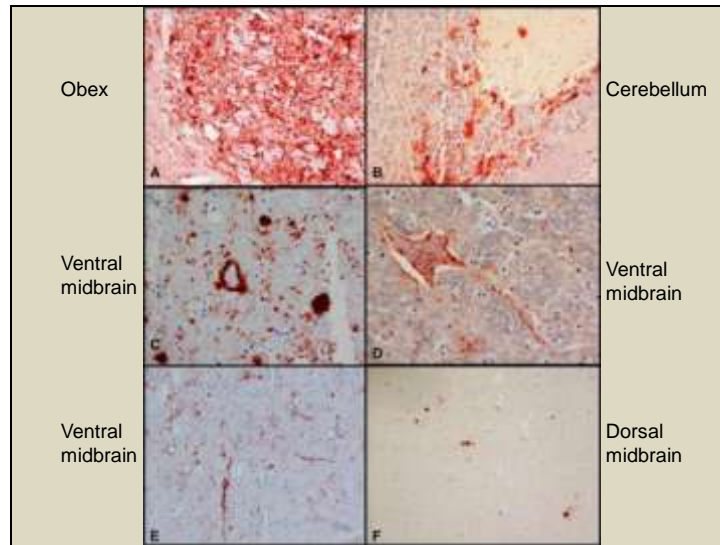
- TeSeE ELISA – positive 8x
- Western blot test for PrP^{res}
- Immunohistochemistry for PrP^{CWD}
- Strong perineuronal labeling in obex (DMNV)
- Variable staining in other nuclei and areas of brain
- Marked labeling in tracheobronchial LN

The medulla oblongata was tested using Bio-Rad's TeSeE ELISA. When the first sample was positive, 6 more samples from the medulla and one from the cerebral cortex were also tested and were also strongly positive.

They also used the Bio-Rad Western Blot test which exhibited bands identical to patterns from an American elk with CWD.

Finally, they conducted IHC on the brain and tracheobronchial lymph nodes. Strong labeling was noted in the obex, particularly around the dorsal motor nucleus of the vagus nerve. Less severely affected nuclei included the spinal tract of the trigeminal nerve, hypoglossal nucleus and the area postrema. Some labeling was seen in the cuneate nucleus, medial lemniscus and the olivary nuclei. Labeling was less prominent in the cerebellum with patchy labeling in some areas, often heavier in the granular layer and moderate in the form of stellate labeling reminiscent of astroglial processes in the molecular layer.

There was marked labeling in the tracheobronchial lymph node.

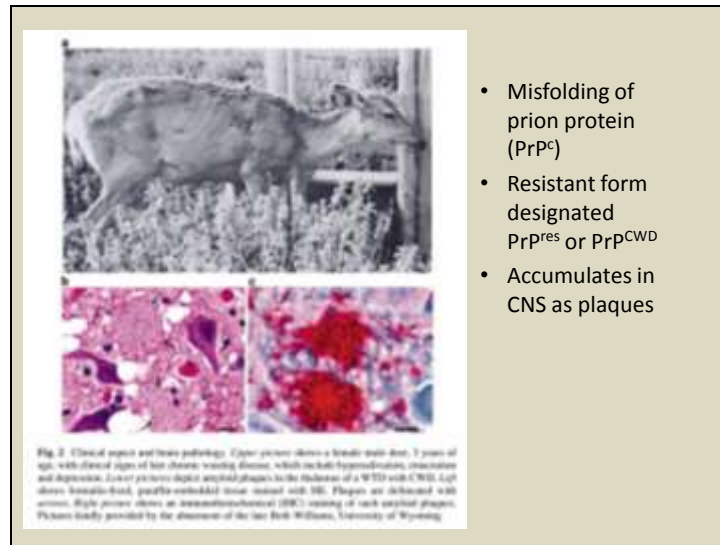


HC labelling of PrP^{CWD} using F89/160.1.5 and 2G11 mAb. A Obex, intense coarse particulate labelling in the DMNV $\times 200$. **B** Cerebellum, patchy labelling in the granular layer and stellate in the molecular layer $\times 200$. **C** Ventral midbrain, scattered granules or accumulations of PrP^{CWD} that appear as plaques $\times 400$. **D** Ventral midbrain, neuronal and axonal labelling $\times 400$. **E** Ventral midbrain, linear type labelling $\times 100$. **F** Dorsal midbrain, sparse immunolabelling, plaque-like accumulation of PrP^{CWD} $\times 100$.

As of January 2017

- Index case reindeer
- 2 elg (moose)
- 2 more reindeer





This caribou essentially exhibited the classic gross and histopathological changes of CWD, as are illustrated in these images taken by the late Beth Williams, who was highly involved in the initial description of this disease. The disease has a very long incubation period, but eventually clinical signs including separation from herd, lowering of head and ears, repetitive walking, hyperexcitability, hypersalivation, emaciation and listlessness occur. Secondary effects include aspiration pneumonia resulting from difficulty swallowing and there is a suggestion that infected cervids can have a greater chance of sudden death following stressful situations, possibly related to exertional myopathy as was seen in this case. As a reminder, CWD is a transmissible spongiform encephalopathy which results from the misfolding of normal prion protein into resistant forms. This protein then accumulates in the central nervous system and other tissues as plaques, disrupting cognitive abilities.

How did it reach Norway?

- Importation of live cervids into Norway is not allowed
- Finland's deer population originates from NA (1934) but no CWD has been identified
- Exposure to sheep with scrapie – Norway has diagnosed a few cases, but not near this herd
- Spontaneous mutation
- Hunting baits



In CWD, prions are shed in urine and feces, which most likely contributes to the horizontal transmission within and between cervid species (John *et al.* 2013). But, commercially produced deer and elk urine from North America, has been freely advertised, sold over the internet and in sporting goods stores, and exported.

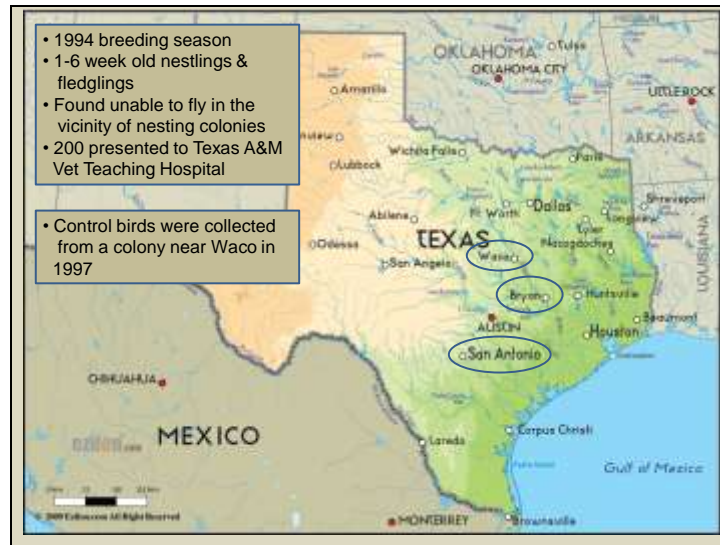
References

- Benestad *et al.* 2016. First case of chronic wasting disease in Europe in a Norwegian free-ranging reindeer. *Vet Res* 47:88.
- John *et al.* 2013. Early detection of chronic wasting disease prions in urine of pre-symptomatic deer by real-time quaking-induced conversion assay. *Prion* 7:253-258.

Expansion of population into
new territory

Metabolic bone disease





“Fledgling and nestling cattle egrets from the Bryan colony, from the last week of June 1994 and until the second week of Aug 1994, were found on the ground unable to fly. Many birds were limping or completely unable to walk, and most drooped one or both wings. The precise number affected was not known; however, over 3,000 dead birds were picked up by the City Sanitation Department in Bryan (Brown, pers. comm.). Observations at the San Antonio colony were made only once, on 4 August 1994. At this time, 100 or more dead juvenile birds were found on the ground.” (Phalen *et al.* 2005).

Birds collected from Waco in 1997 were outwardly normal, age-matched to those from Bryan and San Antonio



FIGURE 1. Lateral radiograph of a fledgling cattle egret with secondary nutritional hyperparathyroidism. The bird was unable to fly. There are folding fractures of the right ulna and radius (black arrow) and a curving deformity of the left radius (white arrow) (Phalen *et al.* 2005).

All birds had signs of bone disease, most of them having fractures. Skeletons were pliable on gross examination.

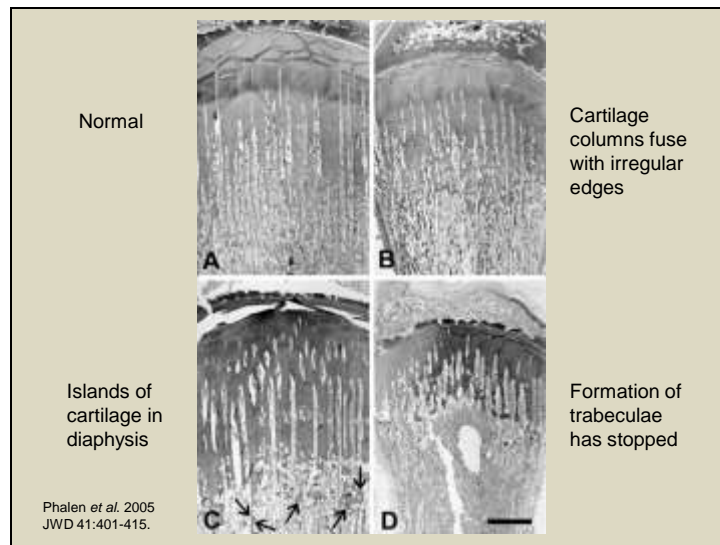


FIGURE 2. Longitudinal section through the proximal tibiotarsus of four fledgling cattle egrets stained with hematoxylin and eosin. Normal growth plate (A), egret from the Waco colony. Note the cartilage columns are straight with parallel sides and that there is an organized transition from cartilage to mineralizing bone. Egret from the Waco colony with secondary nutritional hyperparathyroidism (B). The hypertrophic zone of cartilage is slightly longer than the normal bird. The cartilage columns fuse and have irregular edges, the zone of primary calcification is irregular, and newly formed osteoid seams are thin and discontinuous. Vascular channels are widened. Egret from the Bryan colony with secondary nutrition hyperparathyroidism (C). The zone of primary calcification is similarly irregular, and osteoid seams are thin. In addition, there is persistence of islands of cartilage into the diaphysis (arrows). A second egret with secondary nutritional hyperparathyroidism from the Bryan colony (D). The proliferating and hypertrophic zones of cartilage are markedly shortened, and formation of new trabeculae has stopped. Trabeculae are not found in the medullary cavity. Bar 5

3 mm. (Phalen *et al.* 2005)

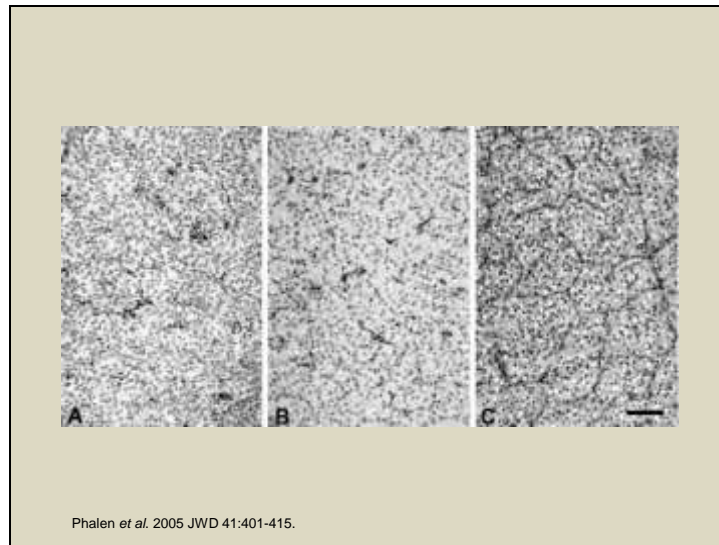


FIGURE 5. Sections of a parathyroid gland from an egret with normally developing bone (A) and the two egrets with fibrous osteodystrophy (B [an egret from Waco] and C [an egret from Bryan]). In panel A, the nuclear-to-cytoplasmic ratio is approximately 1:1. In panels B and C, the parathyroid cells have hypertrophied, causing separation of the nuclei and a decrease in the nuclear to cytoplasmic ratio. Vacuolated cells are absent in the parathyroid from the bird with normal bone, sporadically present in parathyroid from the egret from Waco, and numerous in the parathyroid gland from the egret from College Station. Bar 5 50 mm (Phalen *et al.* 2005).

Stomach content

- The proventriculus and ventriculus of Bryan birds contained 100% insects, primarily crickets and grasshoppers
- Ca^{2+} in grasshoppers = 0.12 – 0.14% (very low)
- Ca^{2+} in crickets = 0.28% (low)
- P in all = 0.65 – 0.81% (normal)
- Reduced Ca^{2+} :P ratio

Why the inappropriate diet?

- Cattle egrets new to North America, arriving in Texas in 1940s
- Initial colonization near river systems, but have pressed into drier habitat
- Rainfall was very low in 1994, reducing vertebrate prey (frog) availability
- Normal diet includes 30% vertebrates, mostly amphibians

Is this an emerging disease?

- What are the drivers of population movement?

References

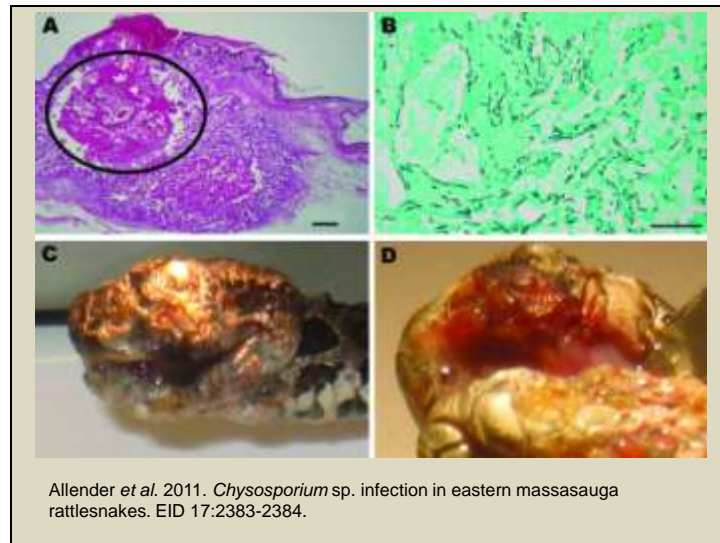
- Phalen *et al.* 2005. Naturally occurring secondary hyperparathyroidism in cattle egrets (*Bubulcus ibis*) from central Texas. *JWD* 41:401-415.

Climate change

Altered pathogen-host dynamics

Snake fungal disease

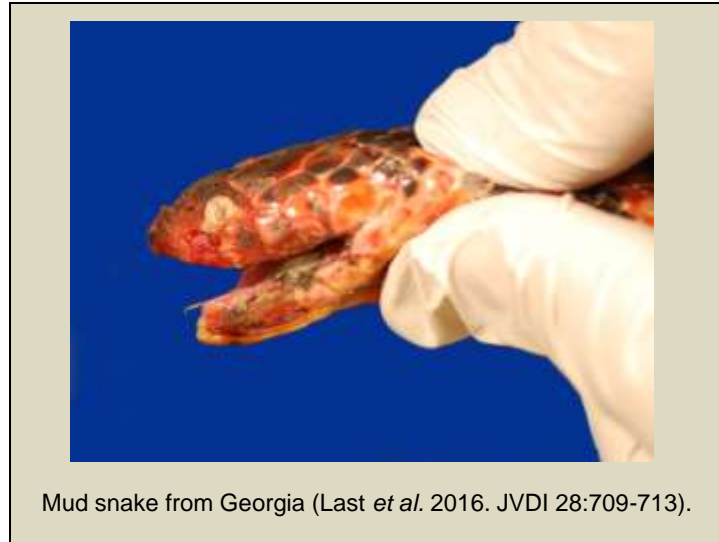




Chrysosporium sp. fungal infection in eastern massasauga rattlesnake (*Sistrurus catenatus catenatus*). C) Facial dermatitis and cellulitis caused by *Chrysosporium* sp. infection in rattlesnake from Carlyle, Illinois, USA; D) close-up showing maxillary fang destruction. A) Maxillary dermal and subcutaneous fungal granuloma (circled area). Hematoxylin and eosin stain, original magnification $\times 2$, scale bar = 500 μm . B) Granuloma center with large numbers of fungal hyphae. Grocott methenamine silver stain, original magnification $\times 10$, scale bar = 100 μm .

Fungi could not be recovered by culture of frozen samples, but PCR did amplify DNA which when sequenced showed >99% homology with *Chrysosporium ophioidicola*. This was an interesting discovery, as around the same time *Chrysosporium* anamorph of *Nannizziopsis vriesii* was also being identified as a primary pathogen of reptiles, in this case in Australia's own bearded dragons.

Slide 63

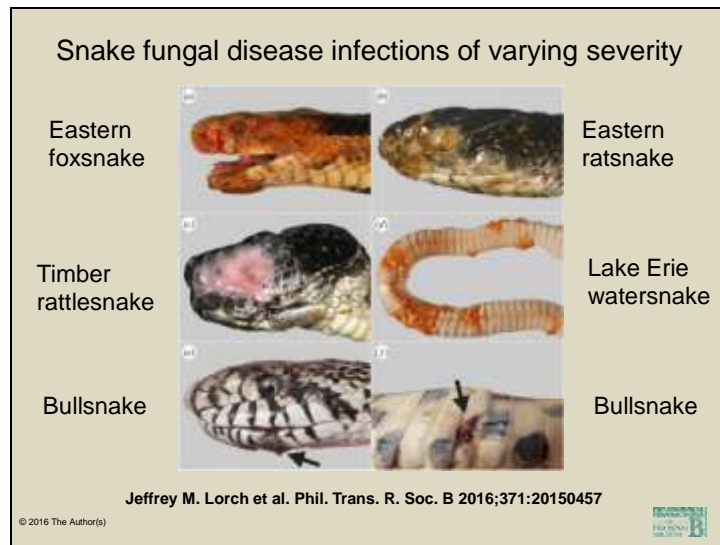


Since these reports, more cases have been published at a fast and furious pace. Here we have a mud snake from Georgia demonstrating marked ulceration and necrosis over the head, affecting the eye and involving the mouth.

Slide 64



The same snake exhibited a section of retained shed adjacent to thickened, pale scales over the dorsum.



Snakes with *Ophidiomyces ophiodiicola* infections of varying severity. Severe infections include (a) eastern foxsnake (*Pantherophis vulpinus*) with disfigured head, (b) eastern ratsnake (*P. alleghaniensis*) with lesions on the eye, snout and lower jaw, (c) timber rattlesnake (*Crotalus horridus*) with skin ulceration and (d) Lake Erie watersnake (*Nerodia sipedon insularis*) with areas of thickened, necrotic skin on ventral surface. Mild infections include bullsnakes (*Pituophis catenifer sayi*) with small lesions on (e) the lower jaw and (f) ventral scale (arrows).

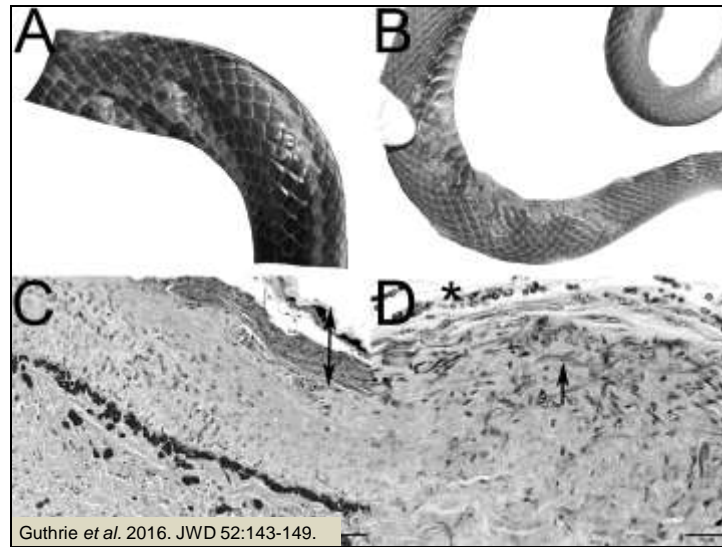
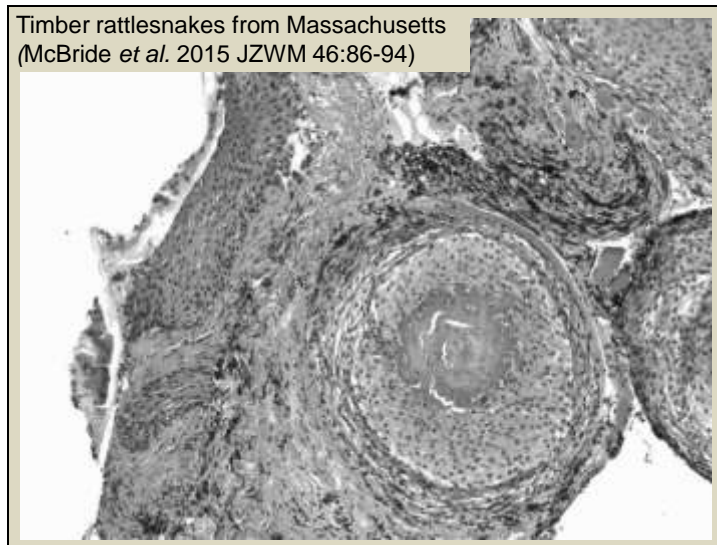


Figure 2. Gross images and histopathology from free-ranging snakes, Virginia, USA, 2014, infected with the fungus *Ophidiomyces ophiodiicola*. (A) Skin, rainbow snake (*Farancia erythrogramma*). Multiple dry, thickened, and slightly raised scales and subcutaneous pustules. (B) Skin, eastern racer (*Coluber constrictor*). Multiple large areas of dry, thickened, and crusty scales. (C) Skin, eastern racer (*Coluber constrictor*). The superficial epidermis is thickened by necrotic debris and mixed inflammatory cells with Periodic acid-Schiff (PAS)-positive fungal hyphae (double arrow). Low numbers of granulocytes and macrophages are present in the dermis. PAS. Bar=50 µm. (D) Skin, northern water snake (*Nerodia sipedon*). The epidermis is replaced by a thick layer of necrotic debris admixed with numerous 2–5 µm in diameter PAS-positive fungal hyphae with parallel to undulating walls and occasional septations (arrow) and branching. Arthroconidia (*) are present on the epidermal surface. PAS. Bar=20 µm.

Slide 67



These timber rattlesnakes from Massachusetts show classic granuloma formation with central necrosis surrounded by macrophages and fibrosis.

Slide 68

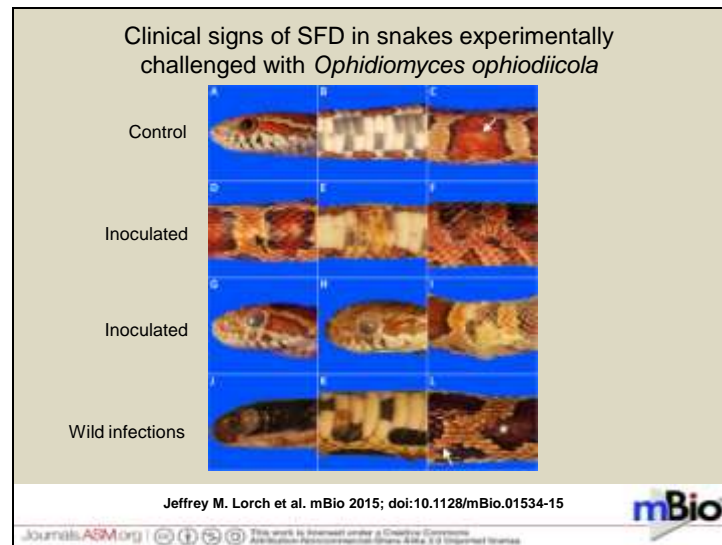


Fungal hyphae are clearly demonstrated with a silver stain.

2011-2016

- The term “snake fungal disease” has become fixed in dialogue
- Original identification of *Chrysosporium ophiodiicola* reassigned to *Ophidiomyces ophiodiicola*
- Koch’s postulates were fulfilled – this is a primary pathogen

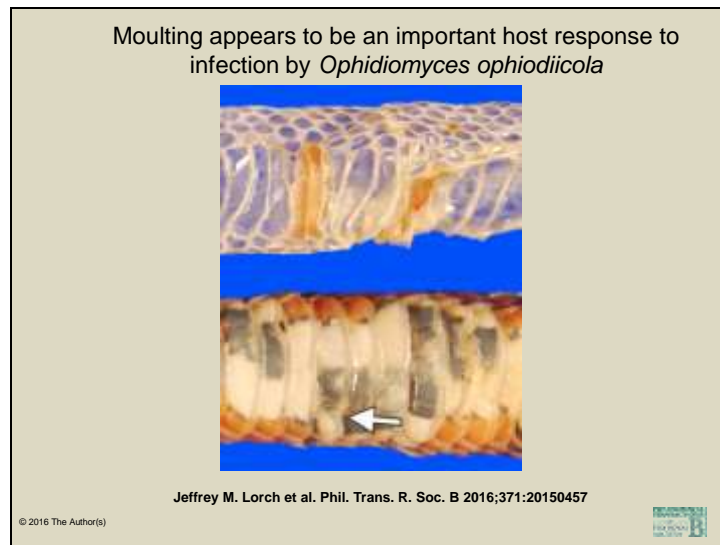
The *Chrysosporium* anamorph of *Nannizziopsis vriesii* complex has been determined to be paraphyletic, which has resulted in transfer of most taxa to other genera, including reassignment of *C. ophiodiicola* to the monotypic genus *Ophidiomyces*.



Two experimental infections have been published. These images are from the paper in which Koch's postulates were fulfilled.

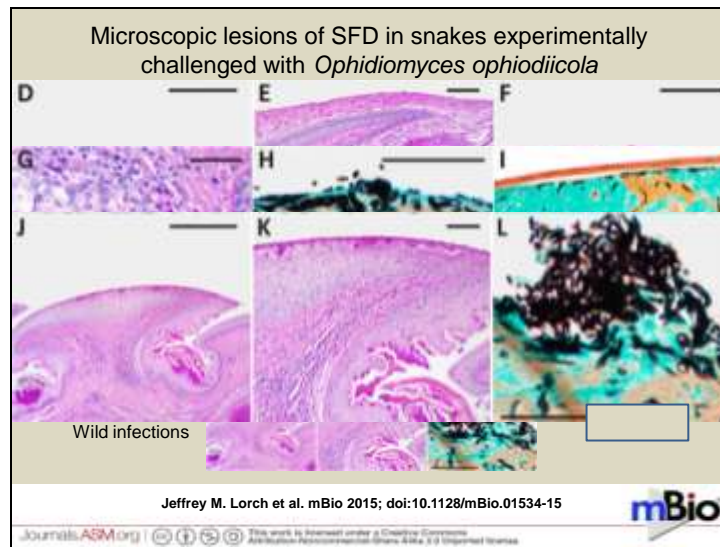
Clinical signs of SFD in snakes experimentally challenged with *Ophidiomyces ophiodiicola*. (A to C) Sham-inoculated sites of snakes in the control group did not develop gross lesions characteristic of SFD. However, subtle damage to the scales (arrow) caused by the abrasion process was visible at the dorsal midbody site. In contrast, snakes exposed to *O. ophiodiicola* developed a range of clinical signs as the disease progressed. (D) Initially, individually infected scales were swollen and whitened (arrow). (E and F) Infected scales later became thickened and turned yellow to brown (E), eventually forming crusts of necrotic skin (F). (G) Infected skin on the snout became similarly thickened and yellow-brown. (H and I) Immediately prior to shedding, fluid accumulated between the old and new layers of skin, causing distortion of the head (H) and vesicle formation at inoculation sites on the body (I). (J to L) The presentations observed in experimentally infected snakes were consistent with those observed in wild snakes diagnosed with SFD at the U.S. Geological Survey National Wildlife Health Center, which often included thickened, yellow-brown areas of skin on the head (J) and ventral scales (K) and edematous scales (arrow) and crusting (asterisk) of the skin (L). (Lorch *et al.* 2015)

In this case the lesions were milder than those often seen in wild cases, but husbandry for these animals was ideal, suggesting a multifactorial basis to severe disease. One of the key points from this infection trial is that lesions generally only developed if the skin was abraded. In the few cases where lesions developed in absence of abrasion, a higher concentration of conidia had typically been applied to the skin.

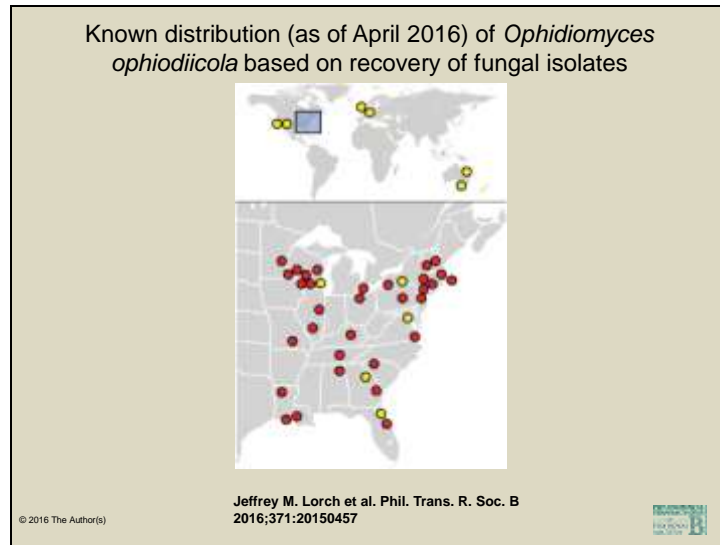


Moulting appears to be an important host response to infection by *Ophidiomyces ophiodiicola*. Most of the infected epidermis (seen here as thickened areas of yellow-brown skin) is cast off with the old skin (top). Post-moult, the skin at the site of a previous lesion is often grossly normal with the exception of some misshapen scales (arrow; bottom).

Key point: Shedding frequency increased. Fungi were generally sloughed with the shed, essentially curing the snake, but in some cases fungal elements were deep enough pre-shed that they remained behind. The authors suggest snakes in the trial may have had the luxury of increasing shedding frequency due to ideal husbandry conditions, but this wouldn't always be the case in the wild.



Microscopic lesions of SFD in snakes experimentally challenged with *Ophidiomyces ophiodiicola*. (A and B) Skin samples from sham-inoculated snakes were within normal limits (PAS stain). Bar, 500 μm (A) or 100 μm (B). (C) Skin samples from sham-inoculated snakes exhibited focal breaks in the stratum corneum attributed to mechanical damage from abrasion; the underlying epidermis was generally within normal limits (PAS stain). Bar, 100 μm . (D and E) Skin samples from snakes exposed to *O. ophiodiicola* developed multifocal superficial epidermal necrosis with extensive epidermal edema (D) and heterophil infiltration and mononuclear to granulocytic dermal inflammation (E) (PAS stain). Bar, 500 μm (D) or 100 μm (E). (F) Breaks in the stratum corneum in infected snakes were most common over areas of epidermal necrosis and granulocytic inflammation, suggesting that infection may be facilitated by preexisting damage to the skin surface (PAS stain). Bar, 100 μm . (G) Some infected snakes developed granulomas consisting of fungal hyphae (arrow) and epithelioid macrophages surrounded by lymphocytes and plasma cells (PAS stain; bar, 50 μm). (H) Areas of epidermal necrosis in snakes exposed to *O. ophiodiicola* often contained 2- to 5- μm -diameter, parallel-walled, septate, branching, fungal hyphae and \sim 2- by 5- μm superficial rectangular arthroconidia (GMS stain). Bar, 50 μm . (I) In a snake preparing to undergo ecdysis, the new stratum corneum can be seen beneath the necrotic epidermis (asterisk) of a lesion. Most fungal hyphae (stained black) are within the older epidermis that will be shed; however, hyphae that have invaded the new epidermis (arrow) may persist after the molt (GMS stain.) Bar, 100 μm . (J to L) Skin samples from free-ranging wild snakes diagnosed with SFD at the U.S. Geological Survey National Wildlife Health Center exhibited lesions similar to those that developed in experimentally infected snakes, including multifocal epidermal necrosis, granulocytic inflammation, and edema (PAS; bar, 500 μm) (J), mixed dermal inflammation (PAS; bar, 100 μm) (K), and fungal hyphae and arthroconidia morphologically consistent with *O. ophiodiicola* (GMS; bar, 50 μm) (L).



Known distribution (as of April 2016) of *Ophidiomyces ophiodiicola* based on recovery of fungal isolates. Yellow dots depict records from captive snakes; red dots represent isolates from wild snakes. Note that some locations in close proximity may be represented by a single dot.

Australian cases were a file snake on display at a crocodile farm in Queensland and a broad-headed snake at a zoo in South Australia. Some of the captive cases pre-date the emergence in wild snakes, with the earliest case dating back to 1985 in a captive ball python in England (Paré and Sigler, 2016)

Affected families (as of April 2016)

- Acrochordidae*
- Boidae
- Colubridae*
- Elapidae*
- Pythonidae*
- Viperidae

* Families represented in Australia

Acrochordidae are the file snakes and the broad headed snake is an elapid.

W5

- Who – lots of wild snake species
- What – fungal dermatitis
- Where – eastern United States
- When – since 2006
- Why – *Ophidiomyces ophiodiicola*
 - But really, why?
 - New release?
 - Changed pathogen?
 - Changed environment?
 - Changed host?

But really, why? – What is the mechanism of emergence? Why is this pathogen emerging?

New release?

- Examination of historical fungal isolates shows that *O. ophiodiicola* was present in captive snakes in the eastern USA since at least 1986. Did it spillover from captive populations?
- “Hibernation blisters” have been reported in wild snakes for decades. Lorch *et al.* (2016) found that 74% of lesions compatible with those described as hibernation blisters were caused by *O. ophiodiicola*. This suggests that the pathogen has been in wild populations for a long time.
- The sequence of documented cases of SFD in wild snakes appears random, separated by 500-1000km, rather than spreading from a point source of spillover.

Changed pathogen?

- Has the fungus gained increased virulence? Again, the seemingly random geographic distribution of documented cases of SFD would not seem to support this hypothesis.

Changed environment?

- The severe outbreak of SFD in timber rattlesnakes in NH in 2006 occurred during a particularly wet year.
- Slight temperature changes during hibernation may be allowing *O. ophiodiicola* to flourish

Changed host?

- Documented outbreaks of severe disease have typically occurred in relatively small or isolated snake populations. These populations may be more closely monitored, explaining greater detection of disease, but they may also be exhibiting reduced genetic diversity and therefore greater susceptibility.

References

- Allender *et al.* 2011. *Chyso sporium* sp. infection in eastern massasauga rattlesnakes. EID 17:2383-2384.
- Guthrie *et al.* 2016. Detection of snake fungal disease due to *Ophidiomyces ophiodiicola* in Virginia, USA. JWD 52:143-149.
- Last *et al.* 2016. Snake fungal disease caused by *Ophidiomyces ophiodiicola* in a free-ranging mud snake (*Farancia abacura*). JVDI 28:709-713.
- Lorch *et al.* 2016. Snake fungal disease: an emerging threat to wild snakes. Phil. Trans. R. Soc. B 371:20150457.
- Lorch *et al.* 2015. Experimental infection of snakes with *Ophidiomyces ophiodiicola* causes pathological changes that typify snake fungal disease. mBio doi:10.1128/mBio.01534-15.
- McBride *et al.* 2015. *Ophidiomyces ophiodiicola* dermatitis in eight free ranging timber rattlesnakes (*Crotalus horridus*) from Massachusetts . JZWM 46:86-94.
- Paré and Sigler. 2016. An overview of reptile fungal pathogens in the genera *Nannizziopsis*, *Paranannizziopsis* and *Ophidiomyces*. J Herp Med Surg. 26:46-53.

Climate change

Altered vector dynamics

Biliary trematode





Through the 20th C., the grey seal population in the Baltic sea has suffered from over-harvesting and reproductive failure due to PCBs. Its level is still far from historic levels and therefore on-going monitoring takes place. Every year, approximately 100-150 seals that have been hunted, caught in fishing gear or found moribund or dead along the Swedish Baltic coast are examined by the Swedish Museum of Natural History.

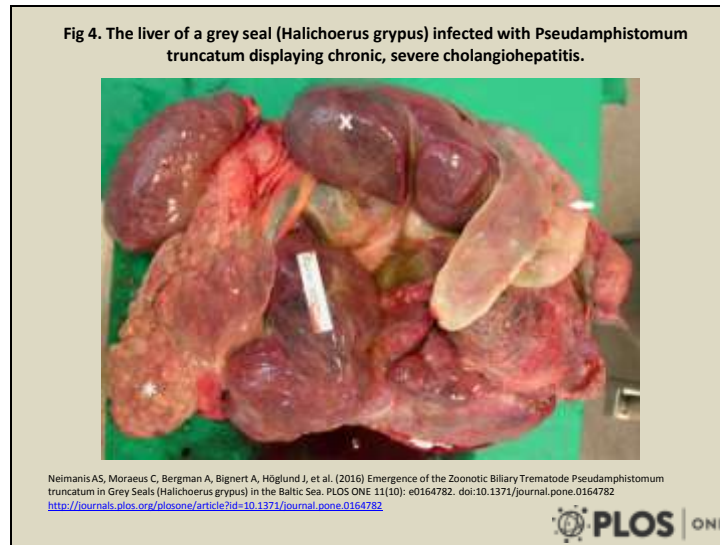
How/why did they notice the increase in biliary fluke?

As is the case when a species is regularly examined in significant numbers over many years, a power set of data is produced which can reveal information which is otherwise inapparent. In this case, there had been no increase in morbidity or mortality to trigger an investigation, but simply an observation that something had changed.



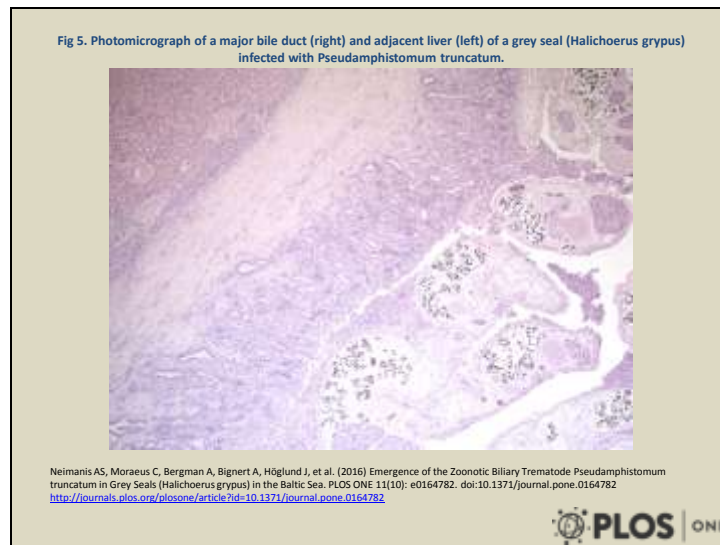
Note the ectatic bile duct filled with beige exudate admixed with 1-1.5mm long, brown trematode parasites centrally. Parasites were found in intrahepatic bile ducts and the gall bladder, but not in the pancreas. Bile duct walls are moderately thickened by chronic inflammation and fibrosis (Neimanis *et al.* 2016).

Often infections were mild and confined to a single liver lobe, but,



In some cases the infection was very severe and widespread involving the whole liver and gall bladder. This is an example of one of the most severely affected cases. Here we can see lobes vary from being markedly atrophic with only severely fibrotic and ectatic bile ducts and intervening connective tissue remaining (*) to being swollen and congested with evidence of hepatic fibrosis and necrosis on cut surface (x). The gall bladder is markedly enlarged and has thick walls (⇔) (Neimanis *et al.* 2016).

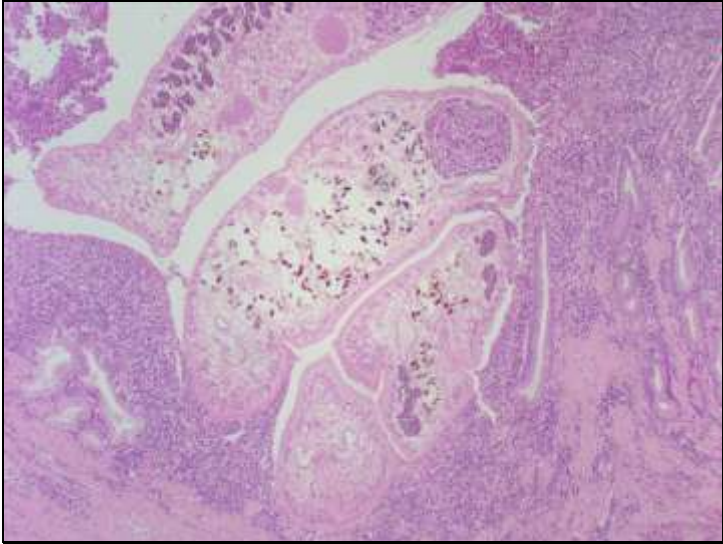
The authors also noted that an enlarged portal lymph node indicated the presence of trematodes.



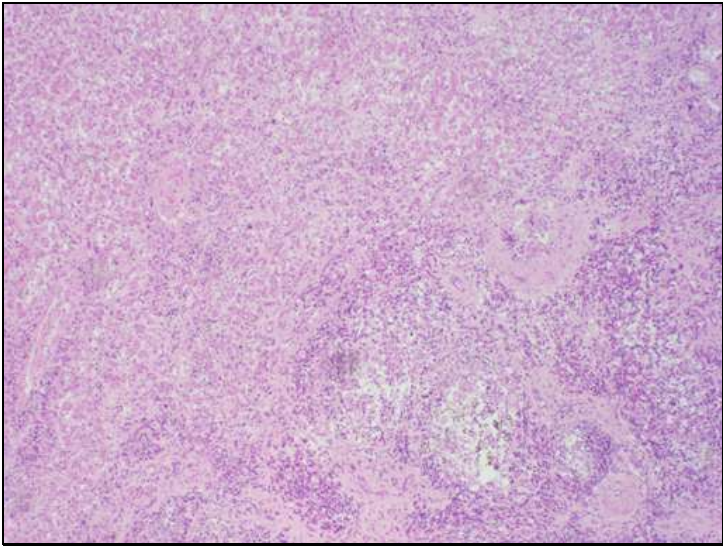
The ductal mucosa is hyperplastic and the duct wall is thickened by fibrosis. Eosinophilic and lymphoplasmacytic inflammation extends through the mucosa, ductal wall and into the adjacent hepatic parenchyma, particularly in portal areas. Cross-sections of numerous adult trematodes are seen within the lumen of the duct. Magnification 40X.

Microscopically, trematodes had a spinous cuticle and their eggs were approximately 25 X 50 μm in size, operculated and had a thick, yellow-brown wall. Associated pathological changes consisted of variable eosinophilic and lymphoplasmacytic cholangiohepatitis, cholangitis and biliary fibrosis (Fig 5). In scattered, more affected areas, hepatic parenchyma was replaced by inflammatory and necrotic debris, often admixed with trematode eggs. In more severely parasitized animals (e.g. ≥ 100 adult flukes), hepatic architecture was effaced by necrosis, inflammation and/or fibrosis and the gall bladder wall was markedly thickened by inflammation, fibrosis and mucosal hyperplasia (Neimanis *et al.* 2016).

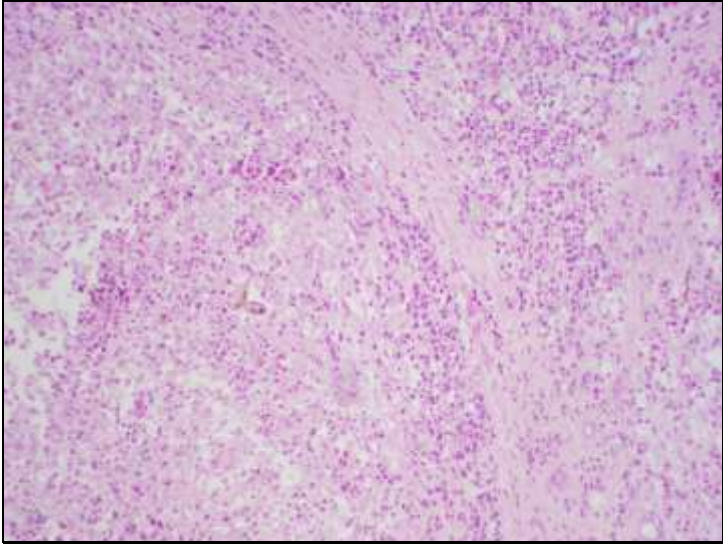
Slide 83

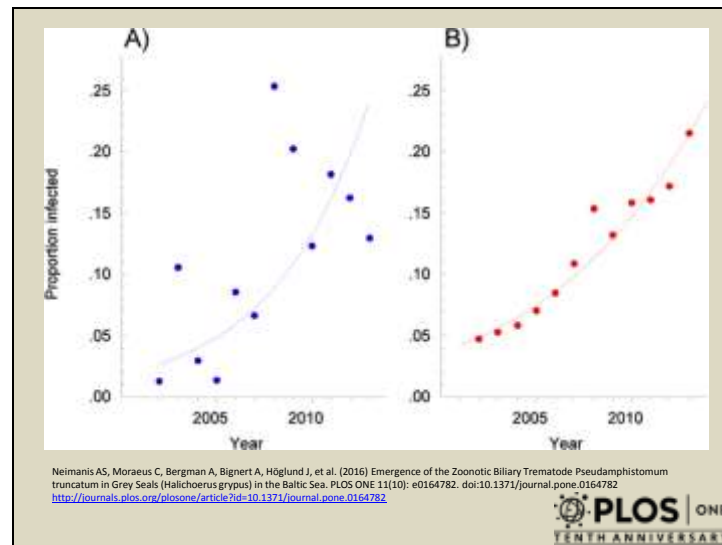


Slide 84



Slide 85





So what's the significance of these flukes in grey seal livers? *P. truncatum* can use almost any fish-eating mammal as its definitive host and the parasite had been found previously in grey seals in this area. However, as we can see in this figure, the incidence has increased significantly since around the turn of the century.

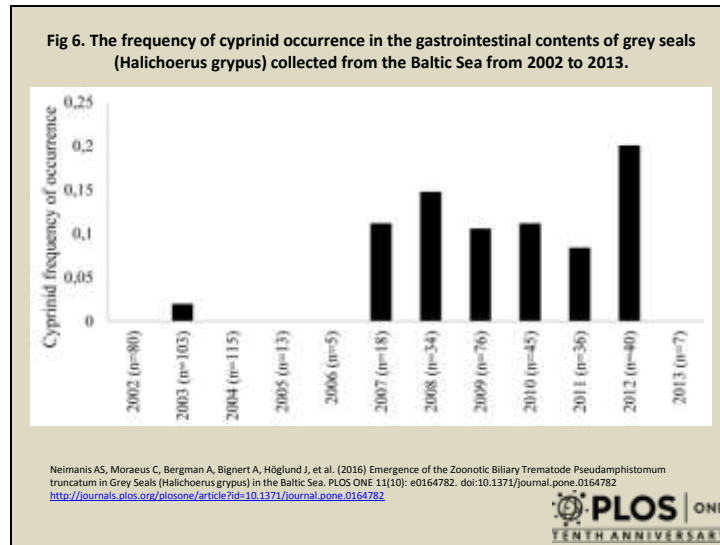
- The first graph shows the raw data. Proportion of grey seals (*Halichoerus grypus*) from the Baltic coast of Sweden infected with *Pseudamphistomum truncatum* per year from 2002 to 2013 unadjusted for explanatory variables. The proportion of infected seals increases significantly over time ($p < 0.01$, log-linear regression) (Neimanis *et al.* 2016).
- Predicted proportion of grey seals from the Baltic coast of Sweden infected with *P. truncatum* per year from 2002 to 2013, adjusted proportions using an average of 8 years of age and observed mean values for sex and cause of death. This reduces the variance in the logistic model ($p < 0.001$, full logistic model compared to intercept only) (Neimanis *et al.* 2016). In addition to seeing an increase in incidence, the authors found that males were significantly more likely to be infected and that young seals and seals caught in fishing gear were significantly less likely to have detectable infections, so when the data are adjusted for these variables, the data smooths out a lot.



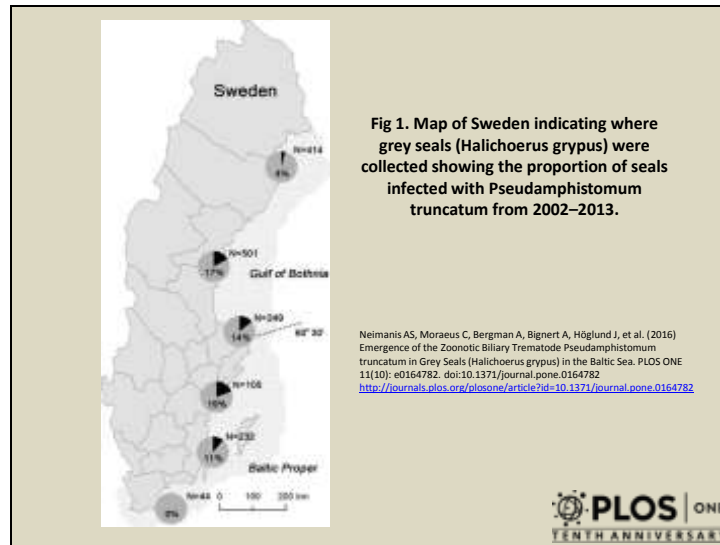
Cyprinid fish, the roach

According to reports produced by HELCOM, the Baltic Marine Environment Protection Commission - Helsinki Commission, which is the governing body of the Convention on the Protection of the Marine Environment of the Baltic Sea Area, roach are now abundant throughout Baltic coastal areas of Sweden and cyprinids as a whole are significantly increasing in the Gulf of Bothnia in the north.

Documented as an intermediate host for *P. truncatum* in other parts of northern Europe.



Luckily, another component of the standardized examinations conducted on the seals is evaluation of gastrointestinal contents. This graph shows that the consumption of cyprinid fish, based on finding hard parts such as otoliths in the gastrointestinal tracts, appears to be increasing, supporting the idea that a cyprinid may be the intermediate host and that they may be increasing in numbers in these areas. Of course, other reasons for prey switching cannot be ruled out.



This map shows the proportion of seals infected with *P. truncatum* based on location. Notice the most southern stretch of coastline has had no infected animals. The sample size here is significantly smaller, so the data need to be interpreted with caution, but the authors suggest that this area of the coast is saltier or less estuarine than the rest of the coast. Roach are a freshwater species, so the salinity in this area may have limited their distribution.

Data are grouped to represent two adjacent counties at once. Pie charts illustrate the proportion of infected seals per total number of animals examined from each pair of counties.

References

- Neimanis *et al.* 2016. Emergence of zoonotic biliary *Pseudamphistomum truncatum* in grey seals (*Halichoerus grypus*) in the Baltic Sea. PLoS ONE 11(10): e0164782. doi:10.1371/journal.pone.0164782